DET NORSKE VIDENSKAPS-AKADEMI I OSLO

GEOFYSISKE PUBLIKASJONER

GEOPHYSICA NORVEGICA

Vol. XXV. No 1 October 1963

KAARE PEDERSEN

On quantitative precipitation forecasting with a quasi-geostrophic model

OSLO 1963
UNIVERSITETSFORLAGET

GEOFYSISKE PUBLIKASJONER

GEOPHYSICA NORVEGICA

VOL. XXV

UTGITT AV
DET NORSKE VIDENSKAPS-AKADEMI
I OSLO

OSLO 1963—65
UNIVERSITETSFORLAGET

GEOFYSISKE PUBLIKASJONER
GEOPHYSICA NORVEGICA
VOL. XXV. NO. 1

ON QUANTITATIVE PRECIPITATION FORECASTING WITH A QUASI-GEOSTROPHIC MODEL

By Kaare Pedersen

FREMLAGT I VIDENSKAPS-AKADEMIETS MØTE DEN 8DE MARS 1963 AV HØILAND

Summary. A method of solving the quasi-geostrophic saturated-adiabatic system of equations, permitting an explicit solution of the vertical velocity produced by the release of latent heat, is presented. The possibility of allowing for the existence of a conditionally unstable layer within the region of condensation is discussed. The method, however, is tested on a highly simplified model in which the lapse rate is saturated-adiabatic within the region of condensation. Two sets of 24-hour forecasts of the precipitation amounts and the heights of the pressure levels 500, 700 and 1000 mb are given; and comparisons of dry- and saturated-adiabatic forecasts are made. The vertical velocity component due to dry-adiabatic motion and the additional vertical velocity produced by the release of latent heat are studied.

The precipitation forecasts obtained from the saturated-adiabatic model compare favorably with the amounts observed, while those obtained from the dry-adiatatic model are too small by a factor of about 3 to 4.

CONTENTS

1. Introduction. Numerous studies have been made in recent years to explore the possibilities of predicting amounts of precipitation over relatively short intervals of time. Most of these experiments have been based upon the quasi-geostrophic system of equations in which the vertical velocity is obtained from a diagnostic ω-equation of the customary type. In some of these studies (e.g., those of SMAGORINSKY, 1956; AUBERT, 1957; and SMEBYE, 1958) comparisons between dry- and saturated-adiabatic models are presented. The prognostic experiments by Smagorinsky and the diagnostic analyses of Smebye gave emphasis to the importance of accounting for the effects of released latent heat, although, even when this effect had been included, the prognostic amounts of precipitation were too small by a factor of about 2 or more.

Aubert, on the other hand, arrived at the rather paradoxical result that, although release of latent heat amplified the vertical motion, the effects on the amount of precipitation were negligible over most of the region. A basic difference between the models used by Smagorinsky and Aubert is due to the circumstance that in the former the amounts of condensed water are directly related to the field of vertical velocity while in the latter they are derived from the equation of continuity of water in the air.

The purpose of the present paper[1] is to re-examine the problem of the role played by released latent heat insofar as large-scale vertical motions and predicted precipitation amounts are concerned. The method here used is akin to that developed by Smagorinsky, although a different approach is used in solving the ω-equation applicable to saturated-adiabatic states.

2. The quasi-geostrophic system of equations. Systems of equations of the quasi-geostrophic type may be developed in a number of ways (e.g., CHARNEY, 1948; FJØRTOFT, 1955; ELIASSEN and KLEINSCHMIDT, 1957; LORENZ, 1960). In the following the derivations will follow the arguments described by Eliassen and Kleinschmidt.

2.1. *The Basic Equations.* Using the quasi-geostrophic relationship first introduced by Hesselberg (1915) and the symbols defined elsewhere, we may write:

$$\boldsymbol{v} = \boldsymbol{v}_g + \frac{1}{f}\boldsymbol{k} \times \left[\frac{\partial \boldsymbol{v}_g}{\partial t} + \boldsymbol{v}_g \cdot \nabla \boldsymbol{v}_g\right] \tag{2.1}$$

The corresponding vorticity equation is then:

$$\frac{\partial}{\partial t} q_g = -\boldsymbol{v}_g \cdot \nabla Q_g - f \nabla \cdot \boldsymbol{v} \tag{2.2}$$

where f in the last term on the right is to be regarded as a constant.

It may be noted here that this form of the vorticity equation satisfies the consistency requirements developed by HOLLMANN (1956), WIIN-NIELSEN (1959) and LORENZ (1960).

[1] The research described in this paper has been sponsored by the Atmospheric Science Program of the National Science Foundation under Grant G-17953 to the University of Chicago.

In a similar measure the thermodynamic energy equation may be written:

$$g\frac{\partial}{\partial t}\frac{\partial Z}{\partial p}=-g\boldsymbol{v}\cdot\nabla\frac{\partial Z}{\partial p}-\sigma\omega-\frac{R}{c_p}\frac{H}{p} \tag{2.3}$$

where σ denotes a measure of the static stability as defined in the list of symbols on page 24.

Introducing the quasi-static equation of continuity of mass

$$\nabla\cdot\boldsymbol{v}+\frac{\partial\omega}{\partial p}=0 \tag{2.4}$$

and the customary approximation to the geostrophic vorticity

$$q_g\approx\frac{g}{f}\nabla^2 Z \tag{2.5}$$

into the vorticity equation, and eliminating the time derivative term between equations (2.2) and (2.3), one obtains the following diagnostic equation in ω:

$$\nabla^2\sigma\omega+f^2\frac{\partial^2\omega}{\partial p^2}=f\frac{\partial}{\partial p}[\boldsymbol{v}_g\cdot\nabla Q_g]-g\nabla^2\left[\boldsymbol{v}\cdot\nabla\frac{\partial Z}{\partial p}\right]-\frac{R}{c_p}\nabla^2\frac{H}{p} \tag{2.6}$$

If, in the thickness advection term, $\boldsymbol{v}$ is identified with the geostrophic wind, the above equations constitute a closed system, except for the unknown heating function.

The heat (H) released by condensation may be given by the formula:

$$H=-L\frac{dr_s}{dp}\left[\frac{dp}{dt}\right]_s \tag{2.7}$$

where (dp/dt) is the individual rate of change of pressure, and subscript s refers to the saturated state.

It is assumed that the inconsistency introduced by incorporating heating and omitting cooling results, for shorter forecasting periods, in relatively small errors.

SMAGORINSKY (1956) outlined a method of solving this saturated-adiabatic system of equations in which he assumed H to be given by

$$H=-\delta L\frac{dr_s}{dp}\omega\,,\qquad \delta=\begin{cases}0 & \text{if } \omega\geqslant 0 \text{ or } r<r_s\\ 1 & \text{if } \omega<0 \text{ and } r=r_s\end{cases} \tag{2.8}$$

In the integration procedure used in connection with quasi-geostrophic models, the time step is usually of the order of one hour; assumption (2.8) may therefore introduce significant errors in cases where the air reaches saturation within this time step. Not only do these errors affect the magnitude of the predicted precipitation, but, since they reduce the scale of the condensation region (which usually is small), they tend also to amplify the truncation errors.

2.2. *The effective vertical velocity.* Since equation (2.6) is linear in the vertical velocity, we may divide it into components. Thus

$$\omega = \omega_A + \omega_H \tag{2.9}$$

where ω_A is the part that corresponds to dry-adiabatic processes, and ω_H may be said to be the additional motion due to the supply of heat.

The general diagnostic equation (2.6) now provides two special equations, viz.,

$$\nabla^2\sigma\omega_A + f^2\frac{\partial^2\omega_A}{\partial p^2} = f\frac{\partial}{\partial p}[v_g\cdot\nabla\, Q_g] - g\nabla^2\left[v\cdot\nabla\frac{\partial Z}{\partial p}\right] \tag{2.10}$$

and

$$\nabla^2\sigma\omega_H + f^2\frac{\partial^2\omega_H}{\partial p^2} = -\frac{R}{c_p}\nabla^2\frac{H}{p} \tag{2.11}$$

Equation (2.11) contains two unknowns, ω_H and H. We now introduce a vertical velocity, ω_E, defined so that

$$\omega_E = \begin{cases} \omega_A & \text{for } \omega_A<0 \text{ and } r=r_s \\ 0 & \text{for } \omega_A\geqslant 0 \text{ or } r<r_s \end{cases} \tag{2.12}$$

We shall refer to ω_E as the effective vertical velocity. For H we may now write

$$H = -L\frac{dr_s}{dp}(\omega_E+\omega_H) \tag{2.13}$$

Form equations (2.11), (2.12) and (2.13) one obtains

$$\nabla^2(\sigma-\sigma_s)\omega_H + f^2\frac{\partial^2\omega_H}{\partial p^2} = \nabla^2\sigma_s\omega_E \tag{2.14}$$

where

$$\sigma_s = \begin{cases} \dfrac{RL}{c_p\, p}\dfrac{dr_s}{dp} & \text{for } \omega_E<0 \\ 0 & \text{for } \omega_E \gtrless 0 \end{cases} \tag{2.15}$$

So far we have only obtained the formal advantage that through equation (2.14) an explicit solution of the vertical velocity produced by the release of latent heat may be found. However, from the knowledge of ω_A through equation (2.10) one may define ω_{Ei} (at pressure level i) by the following equation

$$\omega_{Ei}\Delta t = \omega_{Ai}\Delta_t + \frac{1}{\gamma}(T-T_d)_i\,, \quad \omega_{Ei}\leqslant 0 \tag{2.16}$$

where Δt is the time step and γ is a function of pressure and temperature so that $(T-T_d)_i/\gamma$ expresses the dry-adiabatic lift needed for an air parcel to reach its condensation level. If the ascent (over the time interval Δt) is saturated, $\omega_{Ei}=\omega_{Ai}$. However, if the airparcel reaches the condensation level during the time interval

Δt, ω_{Ei} represents the appropriate fraction of ω_{Ai} that produces condensation. If the airparcel does not reach its condensation level during the time interval Δt, $\omega_{Ei}=0$.

It may be noted that while σ is a measure of the stability for dry-adiabatic ascent, $(\sigma-\sigma_s)$ is a measure of the stability for saturated-adiabatic ascent.

The equation (2.14) is elliptic when everywhere $(\sigma-\sigma_s)>0$. If for some region $(\sigma-\sigma_s)<0$, the equation becomes of the mixed type with both elliptic and hyperbolic regions. It is known that within the troposphere $(\sigma-\sigma_s)$ may be negative in some parts of the condensation regions. This problem does not arise if one uses the primitive system of equations. SMAGORINSKY (1956), therefore, argued that the hyperbolicity was introduced by the quasi-geostrophic assumption. The mathematical formulations of the quasi-geostrophic system of equations presented by AUBERT (1957), SMEBYE (1958) and ELIASSEN (1959) avoid this problem with a mixed-type equation. However, these systems of equations have to be solved by iterative methods, and their convergence has not been properly discussed in the case of atmospheric conditions leading to hyperbolicity of equation (2.14).

Since in the present model the stability is assumed to be quasi-constant, the possibility of hyperbolicity is avoided. Where condensation occurs, $(\sigma-\sigma_s)$ is put equal to zero. In Section 3, however, we will to some extent discuss the possibilities of solutions of a one-dimensional form of equation (2.14) with given boundary conditions, in the case when the equation is of the mixed type.

3. The effect of a conditionally unstable layer within the region of condensation. Since it is known that $(\sigma-\sigma_s)$ may be negative in some parts of the condensation region, it is of interest to obtain a possible solution of the vertical velocity produced by the release of latent heat under such conditions. As an example, let it be assumed:

(i) The air in a vertical column is saturated, having the U.S. Standard Atmospheric lapse rate.

(*ii*)
$$\omega_A(x,y,p)=\omega_{A6}\frac{(p-p_0)(p-p_2)}{(p_6-p_0)(p_6-p_2)}\sin a x \sin by$$

with $\omega_{A6}=10^{-3}$mb sec^{-1}.

The values of σ and σ_s at the centibaric pressure levels are given in Table 1. It is seen that $(\sigma-\sigma_s)$ is negative below 600 mb. Before attempting to solve equation (2.14) directly, let us apply the iterative scheme used by SMEBYE (1958) and ELIASSEN (1959). This method may be described as follows: From equation (2.10) ω_A is obtained. If one knows the temperature and humidity distributions, the amount of heat, H^1, released by condensation produced by ω_A can be computed. The vertical velocity, ω_1, due to this heat, H_1, can be found from equation (2.11). The velocity ω_1 in turn produces a release of latent heat, H_2, which again produces a vertical velocity ω_2. The procedure may be continued further to give an infinite series for ω_H:

(3.1)
$$\omega_H=\omega_1+\omega_2+\omega_3+\cdots\cdots\cdots$$

Table 1. *Representative values of* σ *and* σ_s *corresponding to a saturated U.S. Standard Atmosphere. The units are cgs* $\times 10.^4$

p	σ	σ_s	$\sigma-\sigma_s$
900 mb	0.954	1.32	− 0.366
800 mb	1.18	1.49	− 0.31
700 mb	1.50	1.76	− 0.26
600 mb	1.98	1.85	0.13
500 mb	2.76	1.76	1.00
400 mb	4.13	1.63	2.50
300 mb	6.96	1.43	5.53
200 mb	44.80	0.00	44.80
100 mb	179.00	0.00	179.00

Provided the spatial distribution of the heat sources H_1, H_2, H_3 etc., are similar, differing only in amplitude factors, the series (3.1) must be a geometrical series, ELIASSEN (1959).

With $(a^2+b^2)=k^2$, the equation for ω_1 will be

$$\frac{d^2\omega_1}{dp^2}-\frac{k^2}{f^2}\sigma\omega_1=-\frac{k^2}{f^2}\sigma_s\omega_E \tag{3.2}$$

$$\omega_1(p_2)=\omega_1(p_0)=0$$

The finite difference form of equation (3.2) with the mesh size Δp, becomes

$$A_i(\omega_1)_{i+1}-B_i(\omega_1)_i+C_i(\omega_1)_{i-1}=-D_i \tag{3.3}$$

$$(\omega_1)_0=(\omega_1)_N=0$$

where

$$A_i=C_i=1$$

$$B_i=2+\frac{k^2}{f^2}(\Delta p)^2\sigma_i \tag{3.4}$$

$$D_i=\frac{k^2}{f^2}(\Delta p)^2(\sigma_s\omega_E)_i$$

It is readily seen that for large values of k, the ratio between ω_2 and ω_1 will be larger than unity within the unstable region, and hence the series (3.1) will not converge. However, we must exclude such small-scale motion from our system because of the quasi-geostrophic approximation. Assume the largest k permissible to be $k=k_g=2\pi/l_g$ where $l_g=1000$ km. If for this value of k a bounded solution of ω_H exists, a solution must exist also for all smaller values of k.

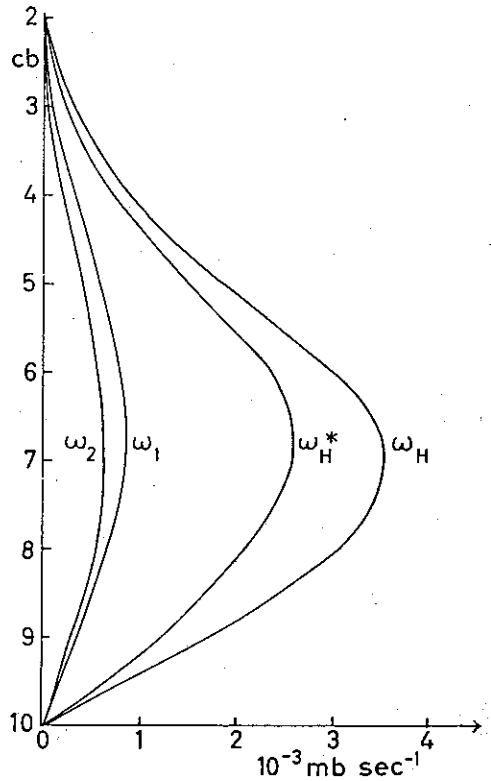

Fig. 1.
The distribution with pressure of ω_1, ω_2,ω_H and ω_H*.
Unit: 10^{-3}mb sec.$^{-1}$

The solutions of ω_1 and ω_2 (assuming no changes in the state of the atmosphere) for $\Delta p = 100$ mb, $f = 10^{-4}$ sec^{-1} and $l = 1000$ km are obtained using a method discovered independently by many people and described by RICHTMYER (1957). The distributions of ω_1 and ω_2 are given in Figure 1. It is seen that for this lapse rate ω_1 and ω_2 have very similar distributions. The total vertical velocity produced by the release of latent heat, ω_H, may therefore be computed from

$$(\omega_H)_i = \frac{(\omega_1)_i}{1-(\omega_2/\omega_1)_i} \tag{3.5}$$

The distribution of ω_H is given in Figure 1.

Seeing that for this particular choice of $(\sigma - \sigma_s)$ a bounded solution of ω_H may be obtained, we return to the mixed type equation (2.14). With assumption (ii), the equation for ω_H will be:

$$\frac{d^2\omega_H}{dp^2} - \frac{k^2}{f^2}(\sigma-\sigma_s)\omega_H = -\frac{k^2}{f^2}\sigma_s\omega_E \tag{3.6}$$

$$\omega_H(p_2) = \omega_H(p_0) = 0$$

The finite difference form of (3.6) will be

$$A_i(\omega_H)_{i+1} - B_i(\omega_H)_i + C_i(\omega_H)_{i-1} = -D_i \tag{3.7}$$

$$(\omega_H)_0 = (\omega_H)_N = 0$$

where A_i, C_i, and D_i are the same as in (3.4), while B_i now is given by

$$B_i = 2 + \frac{k^2}{f^2}(\sigma-\sigma_s)_i\,(\Delta p)^2 \tag{3.8}$$

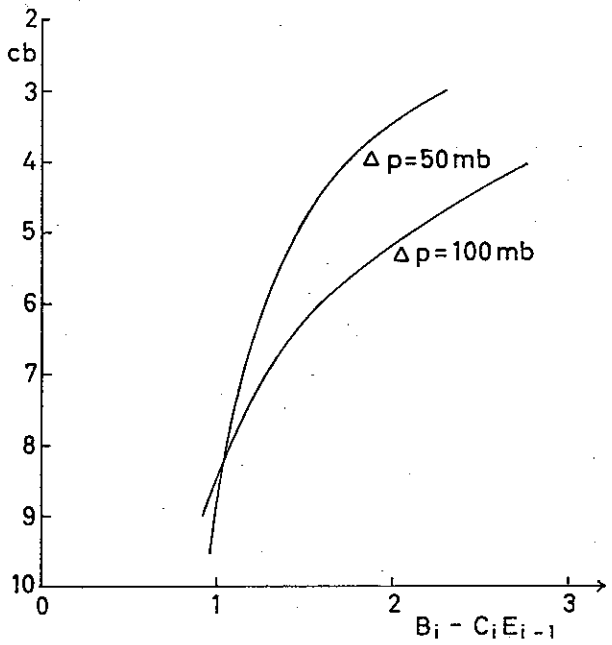

Fig. 2.
Showing the quantity $(B_i-C_iE_{i-1})$ as a function of pressure for $p=100$ and 50 mb.

To assure the existence of a solution of the problem (3.7) it is sufficient to demand that

$$A_i>0\,,\quad B_i>0\,,\quad C_i>0 \qquad (3.9)$$
$$B_i>A_i+C_i$$

The solution of the problem (3.7) is given by

$$(\omega_H)_i=E_i(\omega_H)_{i+1}+F_i\,,\quad (\omega_H)_N=0 \qquad (3.10)$$

where

$$E_i=\frac{A_i}{B_i-C_iE_{i-1}}\,,\quad E_0=0$$
$$F_i=\frac{D_i+C_iF_{i-1}}{B_i-C_iE_{i-1}}\,,\quad F_0=0 \qquad (3.11)$$

It is seen that a necessary condition for a solution of ω_H to exist is:

$$B_i-C_iE_{i-1}>0 \qquad (3.12)$$

The last inequality in (3.9) together with $A_i=1$ (as in the present example), may be shown to give

$$B_i-C_iE_{i-1}\geqslant 1 \qquad (3.13)$$

The inequality $B_i>A_i+C_i$ in (3.9) is therefore a sufficient, but not a necessary, condition. One may conclude that with a limited degree of hyperbolicity a solution of ω_H may exist. With the values of B_i computed from Table 1 with $f=10^{-4}\text{sec}^{-1}$ and $l=1000$ km, the distributions of the function $(B_i-C_iE_{i-1})$ for $\Delta p=100$ mb and for $\Delta p=50$ mb are given in Figure 2. It is evident that the value of $(B_i-C_iE_{i-1})$ will stay positive when $\Delta p\to 0$. The solution of the finite-difference problem (3.7) must therefore approach the solution of the differential problem (3.6) as $\Delta p\to 0$.

The solution of ω_H for $\Delta p=100$ mb and for $\Delta p=50$ mb is the same as that given in Figure 1 (correct to one decimal). For comparison, the solution of ω^*_H with

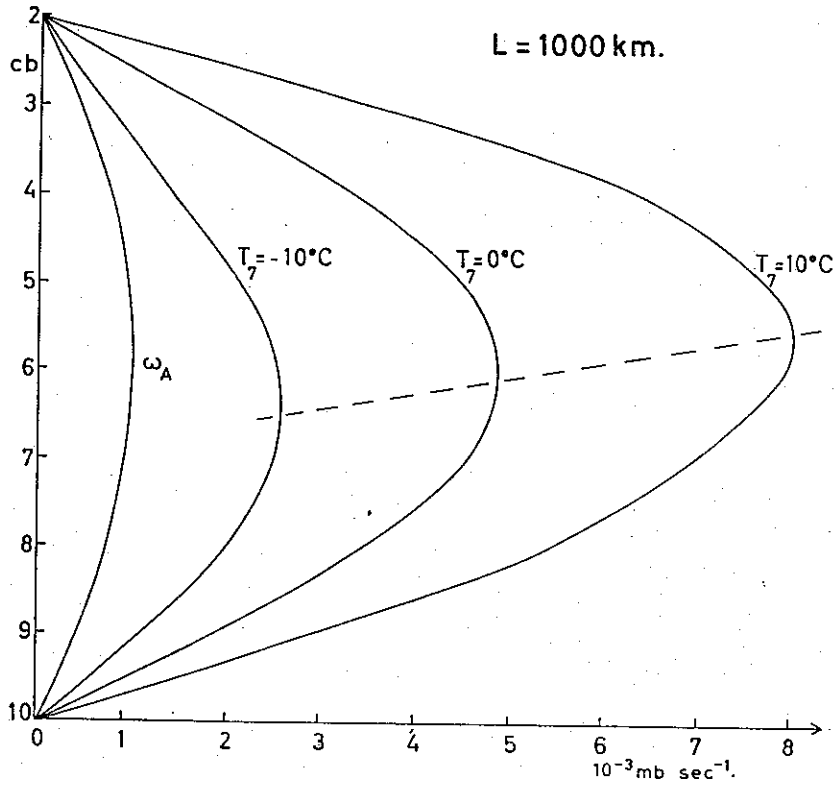

Fig. 3. The vertical velocity, ω_H, as a function of pressure, for saturated-adiabats corresponding to temperatures of −10, 0 and 10°C at the 700 mb level.

$(\sigma-\sigma_s)=0$ below 600 mb, but otherwise the same as in Table 1, is given in Figure 1. It is seen that the unstable region has a significant amplifying effect on the vertical velocity.

When a bounded solution exists in the case where the whole column is saturated, a solution must also exist if only parts of the column are saturated.

It is easily verified that if the lapse-rate is made more unstable than the U.S. Standard Atmosphere, a bounded solution of the problem (3.7) soon ceases to exist. In that case, other influences are necessary to control the motion.

It is difficult to give a general explicit expression for the critical degree of hyperbolicity which may be tolerated in order to obtain a solution of the problem (3.7). In each given case, however, a test of the function $(B_i-C_iE_{i-1})$ as given above may tell wether a solution will exist or not. This test method is equivalent to the following: Regard the finite difference form of the homogeneous differential equation

$$\frac{\partial^2\omega_H}{\partial p^2}-\frac{k^2}{f^2}(\sigma-\sigma_s)\omega_H=0 \tag{3.14}$$

If no non-zero solution of this equation exists that will satisfy the boundary conditions

$$\omega_H(p_2)=\omega_H(p_0)=0 \tag{3.15}$$

then there exists a solution to the nonhomogeneous difference problem (3.7).

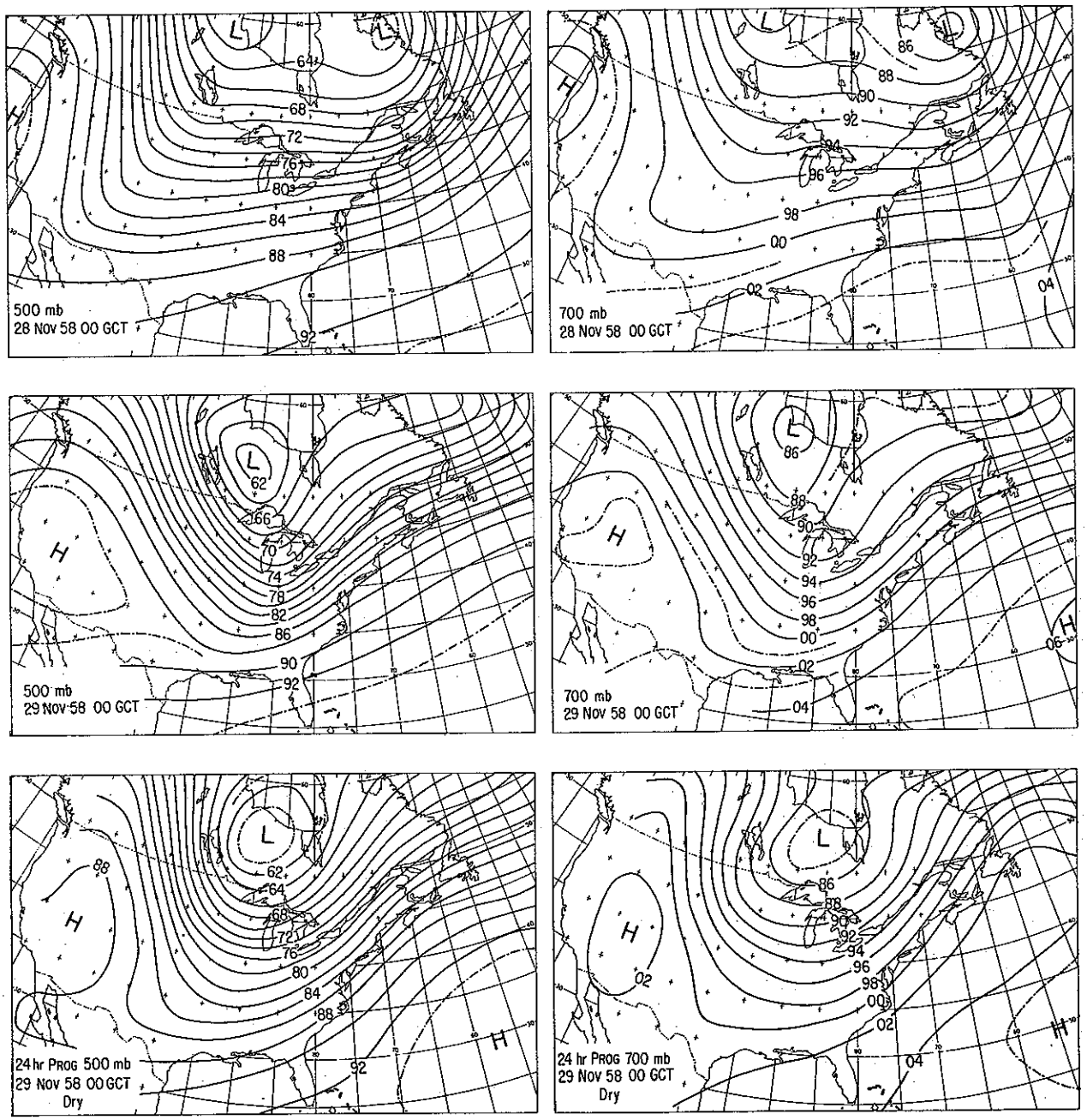

Fig. 4. Upper row: initial maps; center row: verifying maps; lower row: the 24-hour dry-adiabatic forecasts. Unit: 100 feet.

4. A numerical prediction model. 4.1. *Simplifying assumptions.* The method presented in Section 2 has been tested on a highly simplified atmosphere. The following assumptions are made:

(1) Three pressure levels, 1000, 700 and 500 mb, are considered sufficient in describing the state of the atmosphere.

(2) The static stability is quasi-constant.

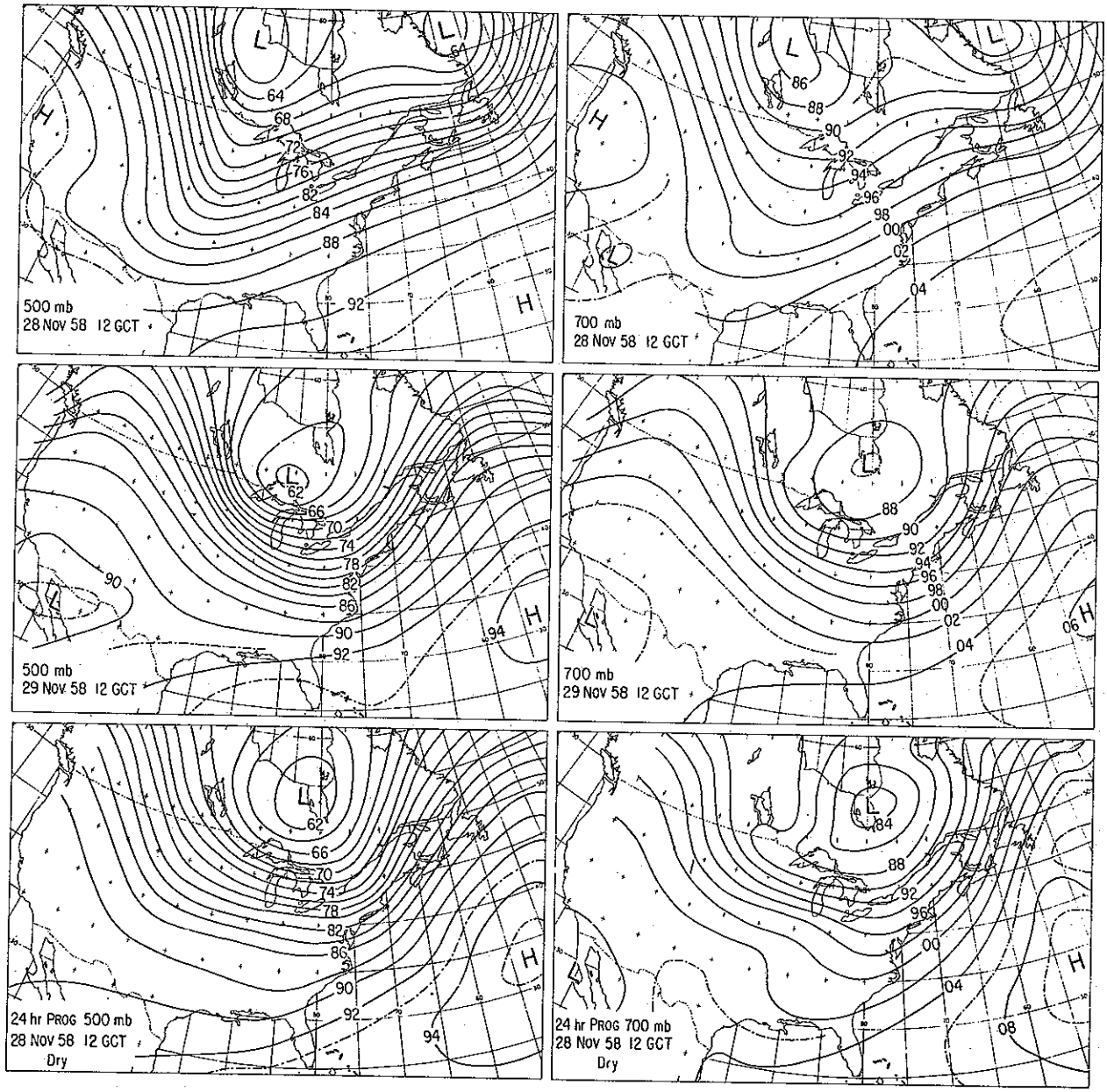

Fig. 5. Same as in Figure 4.

(3) All vertical velocity components have a parabolic profile with zero values at 1000 and 200 mb.

(4) The humidity distribution may be described by the dewpoint depression at the 700 mb level with the vertical gradient locally zero. When saturation is reached at this level, the whole vertical column is assumed to be saturated.

(5) When saturation of a column is reached, the stratification is saturated-adiabatic.

Assumption (4) implies that an unlimited supply of water vapor is available below 700 mb. The decay of a precipitation region cannot therefore be forecast with this atmospheric model.

The writer is aware that some of these assumptions strongly reduce the freedom of the atmosphere in regard to baroclinic instability (e.g., LORENZ, 1960 and MIHALJAN, 1962). Also, the assumptions (4) and (5), together with a given ω_A, determine the profile of ω_H. Since in assumption (3) the distribution of ω_H is said to be parabolic, we may expect some inconsistency between the assumptions. In order to test the consistency, we consider the same type of flow as in Section 3, but this time with a saturated-adiabatic lapse rate. The profile of ω_H for the three saturated-adiabats with 700 mb temperatures of -10°C, 0°C and 10°C are given in Figure 3. The values of f and k are the same as in Section 3. It is seen that, when the temperatures at the 700 mb level within the region of condensation are close to 0°C, the assumptions (4) and (5) agree well with assumption (3).

This test is performed for the single wave length $l = 1000$ km, but for longer waves the shape of the vertical distributions of ω_H will remain essentially unchanged, only the amplitude will vary. For colder atmospheric columns, the precipitation forecast from equation (4.7) will be underestimated due to the assumed parabolic profile of ω_H, and for warmer atmospheric columns, the precipitation forecast will be overestimated.

However, in view of earlier experiments based essentially on the same assumptions (e.g., SMAGORINSKY, 1956 and SMEBYE, 1958) this model atmosphere should be useful for testing short-range precipitation forecasting by the method presented in Sections 2.1 and 2.2, when the temperature at 700 mb meets the requirement stated above.

4.2. *The prognostic equations.* With the assumption (3) in Section 4.1, the vorticity equation (2.2) will be essentially barotropic; it is therefore applied at the 500 mb level where the forecasting ability of the baratropic vorticity equation

$$\frac{\partial}{\partial t} q_5 = -\boldsymbol{v}_5 \cdot \nabla Q_5 + f\left(\frac{\partial \omega}{\partial p}\right)_5 \tag{4.1}$$

has been well established.

From equation (4.1) $\partial Z_5/dt$ is found by relaxation, the boundary condition being $(\partial Z_5/dt) = 0$.

The height of the 700 mb level is obtained through integration of the thermodynamic energy equation between the pressure levels 500 and 700 mb

$$g\frac{\partial}{\partial t} Z_{T_2} = g\int_5^7 \left(\boldsymbol{v}\cdot\nabla\frac{\partial Z}{\partial p}\right)\delta p + \int_5^7 \left(\sigma\omega + \frac{RH}{c_p\, p}\right)\delta p \tag{4.2}$$

where Z_{T_2} denotes the partial thickness of this layer.

From assumption (3) in Section 4.1, the height of the two pressure levels, 500 and 700 mb, can determine our system of equations. Tests indicate, however, that it is more satisfactory to estimate the right-hand side of the equation (2.10) through integration over the deeper layer 500—1000 mb. The height of the 1000 mb level is obtained by integration of the thermodynamic energy equation between 700 and 1000 mb:

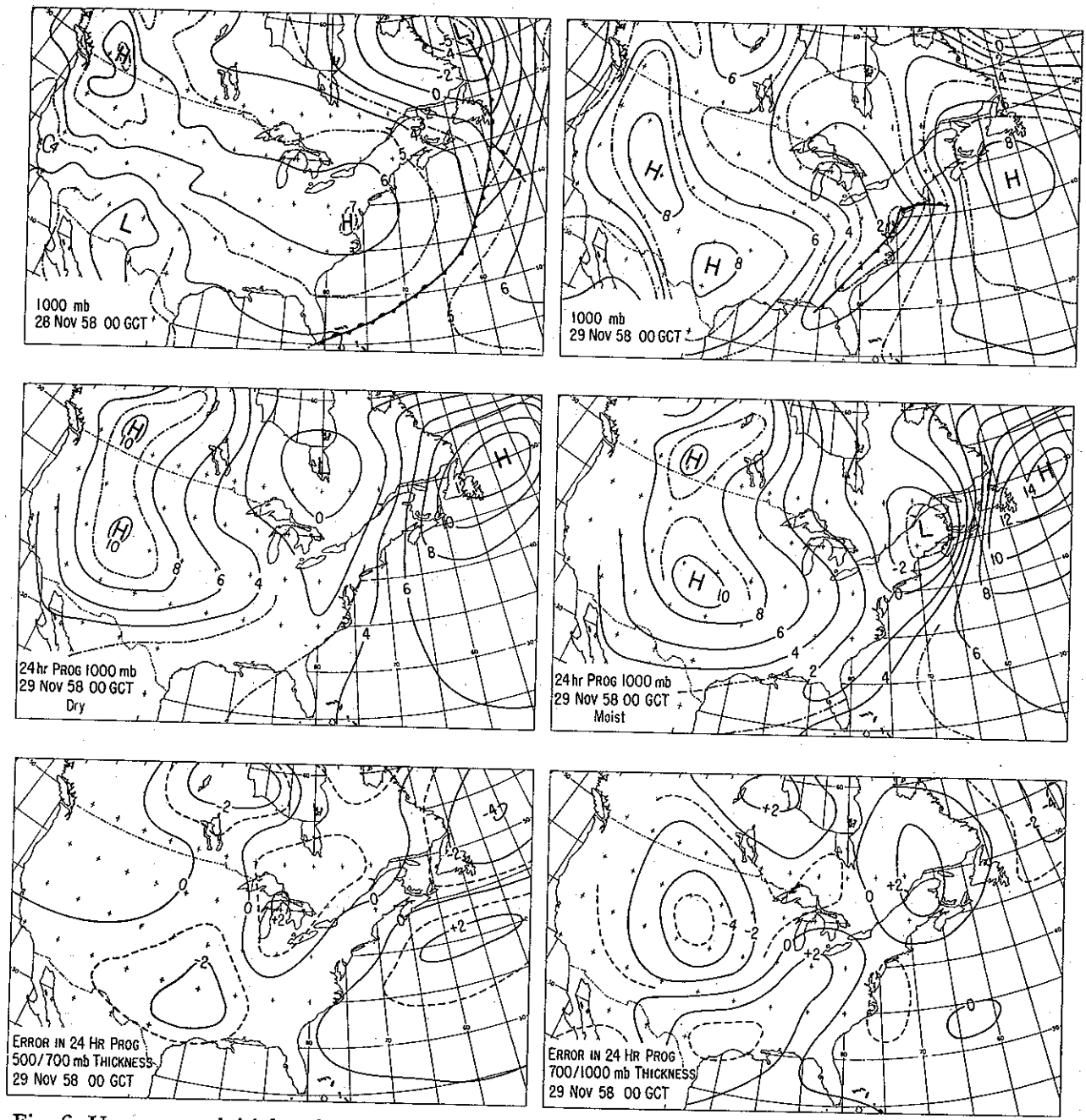

Fig. 6. Upper row: initial and verifying maps; center row: the 24-hour dry- and moist-adiabatic forecasts; lower row: error maps of the partial thicknesses.

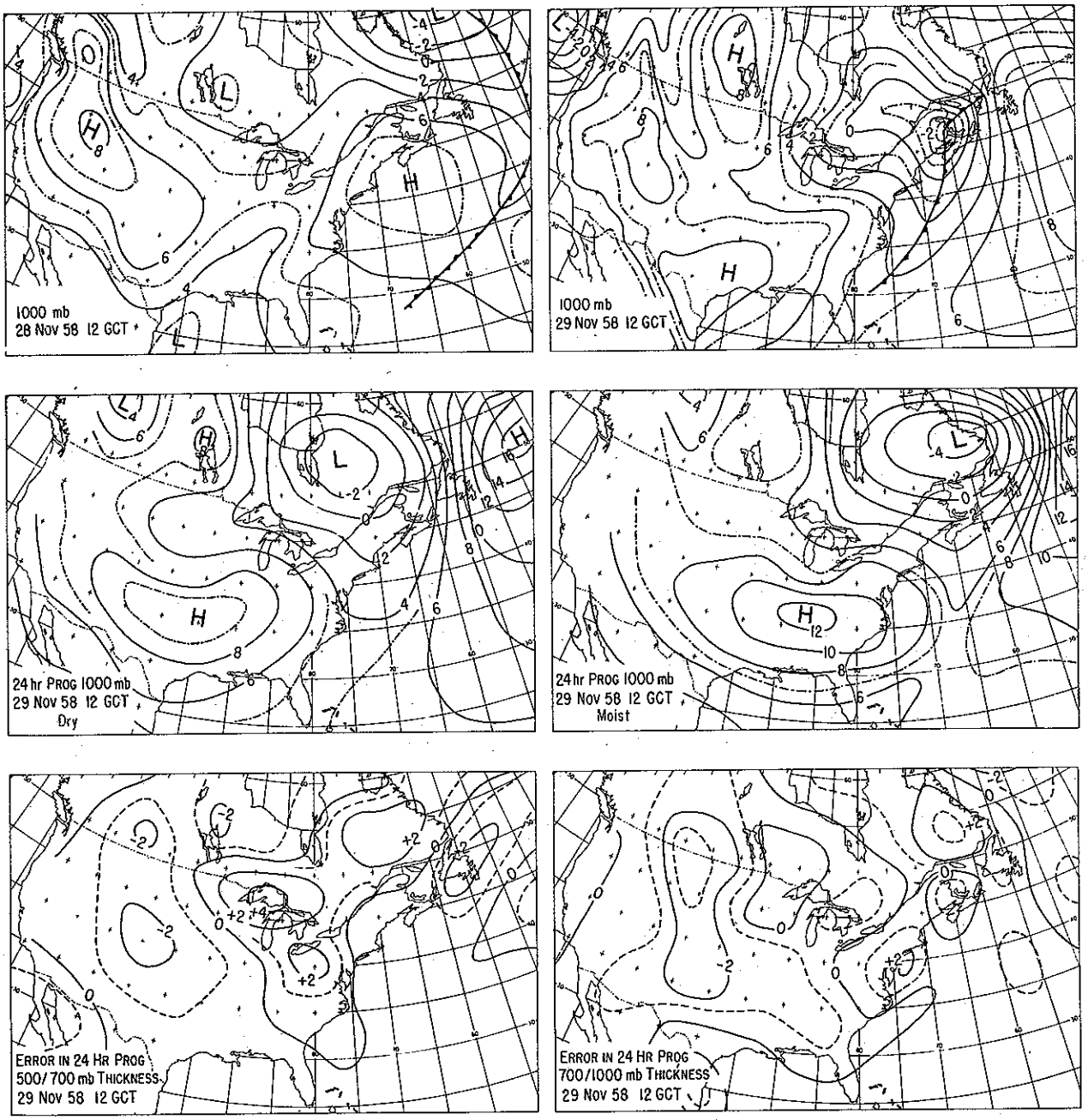

Fig. 7. Same as in Figure 6.

$$g\frac{\partial}{\partial t}Z_{T_1} = g\int_7^0\left(v\cdot\nabla\frac{\partial Z}{\partial p}\right)\delta p + \int_7^0\left(\sigma\omega+\frac{RH}{c_p p}\right)\delta p \tag{4.3}$$

where Z_{T_1} denotes the partial thickness of this layer. The horizontal thickness advection terms in equation (4.2) and (4.3) are approximated by

$$g\int_5^7\left(v\cdot\nabla\frac{\partial Z}{\partial p}\right)\delta p = -gv_{g_7}\cdot\nabla Z_{T_2}$$

$$g\int_7^0\left(v\cdot\nabla\frac{\partial Z}{\partial p}\right)\delta p = -gv_{g_7}\cdot\nabla Z_{T_1} \tag{4.4}$$

Accepting the assumptions in Section 4.1, the last term in equation (4.2) and (4.3) may be written:

$$\int_5^7\left(\sigma\omega+\frac{RH}{c_p p}\right)\delta p = \begin{cases}\hat{\sigma}_2\int_5^7(\omega_A+\omega_H)\delta p & \text{for } \omega_E = 0\\ \hat{\sigma}_2\int_5^7(\omega_A-\omega_E)\delta p & \text{for } \omega_E<0\end{cases}$$

$$\int_7^0\left(\sigma\omega+\frac{RH}{c_p p}\right)\delta p = \begin{cases}\hat{\sigma}_1\int_7^0(\omega_A+\omega_H)\delta p & \text{for } \omega_E = 0\\ \hat{\sigma}_1\int_7^0(\omega_A-\omega_E)\delta p & \text{for } \omega_E<0\end{cases} \tag{4.5}$$

$\hat{\sigma}_1$ and $\hat{\sigma}_2$ being defined by the above equations (4.5).

The dewpoint depression at 700 mb is predicted from

$$\frac{\partial}{\partial t}(T-T_d)_7 = -v_{g_7}\cdot\nabla(T-T_d)_7+\tau\omega_7\,,\quad (T-T_d)_7\geqslant 0 \tag{4.6}$$

This equation is obtained from a combination of the thermodynamic energy equation and the equation for the continuity of water vapor, both applied at a pressure level and for the region of no condensation only. The quantity τ is a function of the lapse rate and of the vertical distribution of water vapor. Under the assumption that the vertical gradient of dewpoint depression is locally zero, CARLSTEAD (1959), the value of $\tau=\gamma=8.5°C/cb$.

Since we have to apply the geostrophic approximation for the horizontal wind, it is a great advantage not to have to forecast explicitly the water vapor content in the regions of condensation.

Omitting the water vapor above 400 mb, the precipitation per time step, ΔN, becomes

$$\Delta N = \begin{cases}\left[\int_4^0(\omega_E+\omega_H)\frac{dr_s}{dp}\frac{\delta p}{g}\right]\Delta t & \text{for } \omega_E<0\\ 0 & \text{for } \omega_E = 0\end{cases} \tag{4.7}$$

r_s at 700 mb is determined by a semi-empirical relation to the partial thickness, the vertical variation of r_s is as in assumption (5) in Section 4.1.

4.3. *The diagnostic equations.* Integration of the equation (2.10) between the pressure levels 500 and 1000 gives the following equation for the dry-adiabatic velocity component:

$$\hat{\sigma}\int_5^0 \nabla^2\omega_A\delta p+f^2\int_5^0\frac{\partial^2\omega_A}{\partial p^2}\delta p=f[(v_g\cdot\nabla Q_g)_0-(v_g\cdot\nabla Q_g)_5]+g\nabla^2[v_{g_7}\cdot\nabla(Z_{T_1}+Z_{T_2})] \tag{4.7}$$

The effective vertical velocity is computed from

$$\omega_{E_7}=\omega_{A_7}+\frac{1}{\gamma\Delta t}(T-T_d)_7\,,\quad \omega_{E_7}\leqslant 0 \tag{4.8}$$

From assumptions (3), (4) and (5), the equation for the vertical velocity produced by the release of latent heat becomes extremely simplified. The best estimate of ω_H is probably obtained by integrating equation (2.14) between the pressure levels 500 and 1000 mb. In regions where $\omega_E>0$ the equation for ω_H becomes

$$f^2\int_5^0\frac{\partial^2\omega_H}{\partial p^2}\delta p=\nabla^2\int_5^0\sigma_s\omega_E\delta p\,,\quad \omega_E<0 \tag{4.9}$$

σ_s is found from equation (2.15). In regions where $\omega_E=0$, ω_H is given by

$$\hat{\sigma}\int_5^0\nabla^2\omega_H\delta p+f^2\int_5^0\frac{\partial^2\omega_H}{\partial p^2}\delta p=\nabla^2\int_5^0\sigma_s\omega_E\delta p \tag{4.10}$$

The right-hand side is non-zero only for gridpoints that are next to those where condensation occurs.

Equations (4.7) and (4.10) are solved by relaxation, the lateral boundary conditions being

$$\omega_A=0,\quad \omega_H=0 \tag{4.11}$$

For equation (4.10) the boundary conditions around the condensation areas are given by equation (4.9).

5. Results of the numerical integrations. The simplified vorticity equation (4.1) is not able to forecast realistically the very long waves, therefore a limited forecasting area must be used. The integrations were performed over the area between 30°—120°W and 10°—68°N. A Mecator map projection was used with a mesh size equal to 5° latitude at equator (19 × 18 grid points). With a one-hour iteration period, the computing time for a saturated-adiabatic 24-hour forecast was 14 minutes on an IBM-704 computer.

Since energy was introduced on a small scale by the released heat, it proved necessary to apply a smoothing operator at the 700 and 1000 mb levels. This reduced

the energy on wavelengths smaller than four times the mesh size. No smoothing was applied at the 500 mb level. In later time steps (after 12 hours) a smoothing of ω_H was introduced. This smoothing, however, proved unnecessary and should not have been applied.

The synoptic situations selected for study were chosen on the basis of the observed precipitation. On 28 November 1958, a widespread precipitation area moved across the eastern half of the United States. It should also be noted that within the condensation regions the temperatures at 700 mb were close to 0°C. Twenty-four-hour predictions were made, based on initial data at 28 November 1958, 00 GCT and 28 November 1958, 12 GCT. Three numerical experiments were carried out:

(1) The stability parameters $\hat{\sigma}_1$, $\hat{\sigma}_2$ and $\hat{\sigma}$ were kept constant. The value of each parameter was put equal to its mean value over the area at the initial time.
(2) The values of $\hat{\sigma}_1$, and $\hat{\sigma}_2$ were allowed to vary as functions of the partial thicknesses in the thickness equations (4.2) and (4.3) on the scales larger than four times the mesh size, while $\hat{\sigma}$ in the ω_A-equation was constant. This is permissible since on the larger scales the term including $\hat{\sigma}$ in the ω_A-equation becomes relatively small. The effect of this variation was to reduce the errors on the larger scales in the thickness forecast by about 100 feet in 24 hours.
(3) A horizontal eddy-diffusion term as proposed by RICHARDSON (1926) was introduced. The effect was significant on the forecasts of dewpoint depression and precipitation amounts.

Unless otherwise mentioned, the variation in stability and the eddy-diffusion are included in the forecasts presented here.

5.1. *Prognoses of pressure levels.* The initial and verifying synoptic situations of the 500 and 700 mb heights, and the 24-hour forecasts obtained by the dry-adiabatic model, are shown in Figures 4 and 5. North of about 35°N, cyclonic vorticity is computed farther to the northeast than was observed, south of about 35°N the trough is predicted to be slightly west of the observed position. These types of errors are also recognized in the 700 mb forecasts. Ageostrophic motion may account to some extent for both these errors; north of about 35°N, because of the cyclonic curvature of the flow, the geostrophic wind is an overestimation of the true wind, south of about 35°N this error is more than compensated for by lack of the proper effect of the Hadley cell type of circulation and of turbulent vertical transport of westerly momentum.

The forecasts of the 500 mb level with the saturated-adiabatic model are not significantly different from the dry-adiabatic forecasts. This simply means that the divergence term as treated by this model is very small. At 700 mb, the difference between the two models becomes noticeable. However, the difference is best seen at the 1000 mb level. The synoptic situation at 1000 mb at the initial and verifying times is given in Figures 6 and 7, together with the 24-hour forecasts with the dry- and saturated-adiabatic model. Also shown in these Figures are the errors in the partial thicknesses

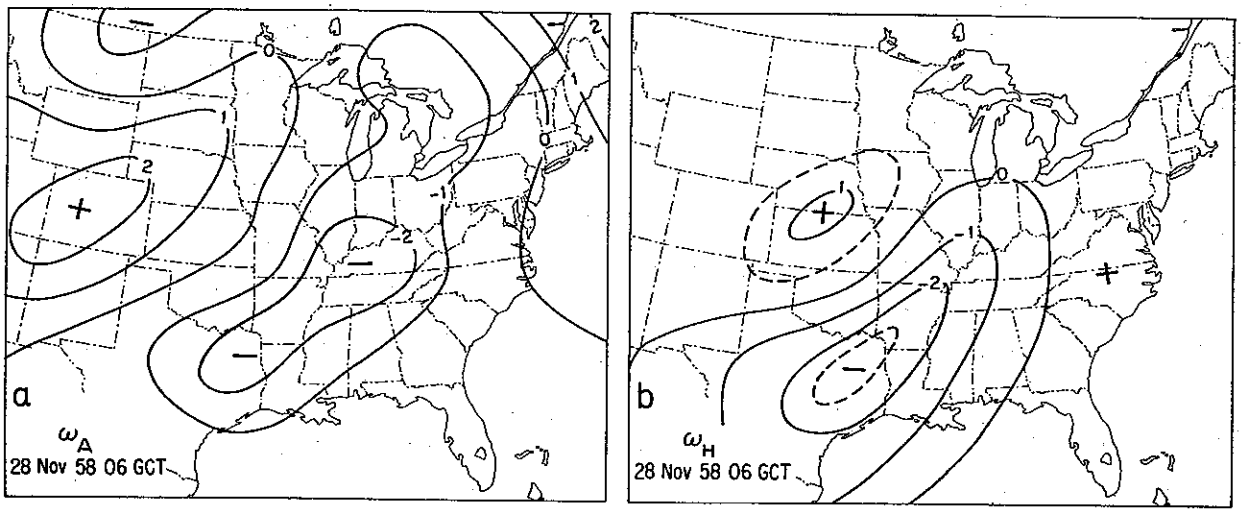

Fig. 8. (a) Six-hour forecasts of ω_A obtained from the saturated-adiabatic model. Unit: 10^{-3} mb sec^{-1}.
(b) Six-hour forecast of ω_H. Initial data 28 November 1958, 00 GCT.

as forecast with the dry-adiabatic model. As observed by AUBERT (1957), the saturated-adiabatic model gives a marked intensification of the cyclone at lower levels, and an increased speed of propagation of the surface cyclone.

The greatest error in the 1000 mb forecasts is the overestimation of the build-up of the anticyclone over the Atlantic on the east coast of the United States. This error is reflected in the forecasts of both the 500/700 and the 700/1000 mb thicknesses. The air entering the Atlantic region is rather cold, and computations show that the sensible heat flux from the warmer ocean is quite considerable. The effect of this flux on the thickness pattern is discussed by PETTERSSEN, BRADBURY and PEDERSEN (1961). Assuming that the divergence produced by the flux of sensible heat is negligible at the 500 mb level, estimates of the type described by Petterssen et al indicate that about half the error in the anticyclone build-up may be due to the omission in the integrations of the sensible heat flux.

Table 2. *Some statistical parameters for the dry-adiabatic forecasts.*

		Skill score	Persistency	Correlation between tendencies	Root mean square change	Root mean square error
24-hr. prog.	1000 mb	.73	.05	.91	360 ft.	230 ft.
based on 28 Nov. 1958	700 mb	.55	.88	.90	300 ft.	222 ft.
00 GCT	500 mb	.69	.94	.90	358 ft.	216 ft.
24-hr. prog.	1000 mb	.83	— .10	.84	371 ft.	214 ft.
based on 28 Nov. 1958	700 mb	.84	.83	.89	340 ft.	199 ft.
12 GCT	500 mb	.65	.89	.85	484 ft.	303 ft.

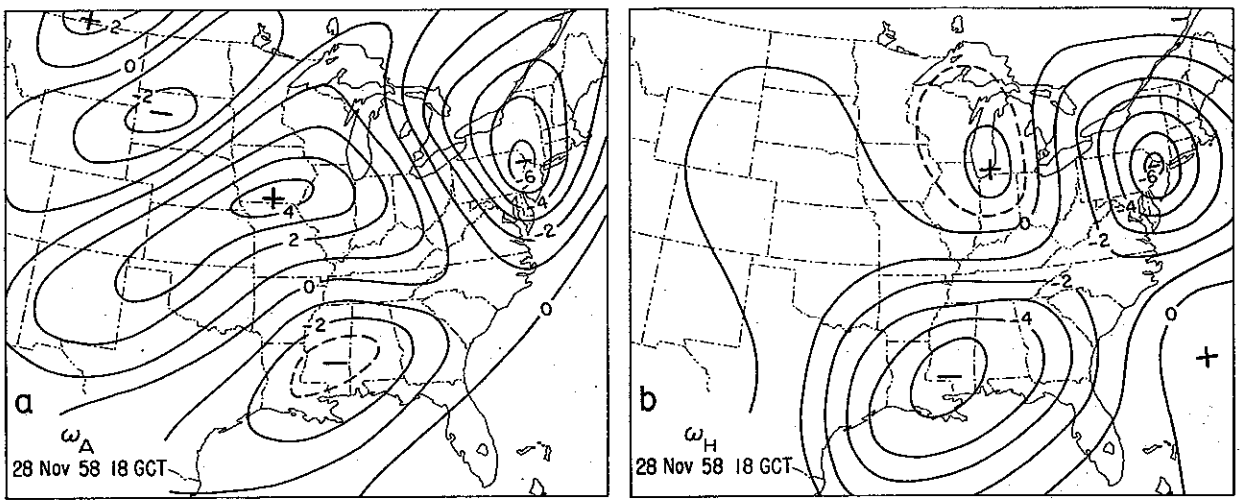

Fig. 9. (a) Eighteen-hour forecast of ω_A obtained from the saturated-adiabatic model.
(b) Eighteen-hour forecast of ω_H. Initial data 28 November 1958, 12 GCT.

Some statistical parameters for the 24-hour forecasts for nine times eight gridpoints in the center of our forecasting region are given in Table 2. These values are for the forecasts obtained by the dry-adiabatic model with varying stability on the larger scales. For the saturated-adiabatic model, the skill score and the correlation coefficient between observed and computed tendencies was the same as with the dry-adiabatic model, even though the root mean square error was slightly larger.

5.2. *Prognoses of vertical motion and precipitation.* Distribution of the dry-adiabatic component, ω_A, and the component due to release of latent heat, ω_H, as computed with the saturated-adiabatic model, are shown in Figures 8a, 9a and 8b, 9b respectively. The velocities given in Figures 8a and b are 6-hour forecasts based on initial data 28 November 1958, 00 GCT. Figures 9a and b show 18-hour forecasts based on the same initial data. It is interesting to note that, after the precipitation area splits, the ratio between ω_H and ω_A for the southern part is about 2, while for the northern part it is close to 1. Although the two areas have about the same horizontal scale, the southern area is warmer, and the value of σ_s in equation (4.9) is therefore greater to give a larger value of ω_H relative to ω_A. The slight inconsistency between Figures 9a and b is due to the smoothing of ω_H.

The observed 24-hour precipitation amounts, together with those computed with the saturated- and dry-adiabatic models, are given in Figure 10. The amounts computed without eddy diffusion are shown in Figure 11.

For this particular case, the saturated-adiabatic model is seen to give precipitation amounts similar to those observed, while the dry-adiabatic model gives amounts too small by a factor of 3—4. In comparing the precipitation amounts predicted with both these models, it should be remembered that, because of the intensification of the cyclone in the saturated-adiabatic model, its dry-adiabatic velocity component is somewhat larger than the vertical velocity in the dry-adiabatic model.

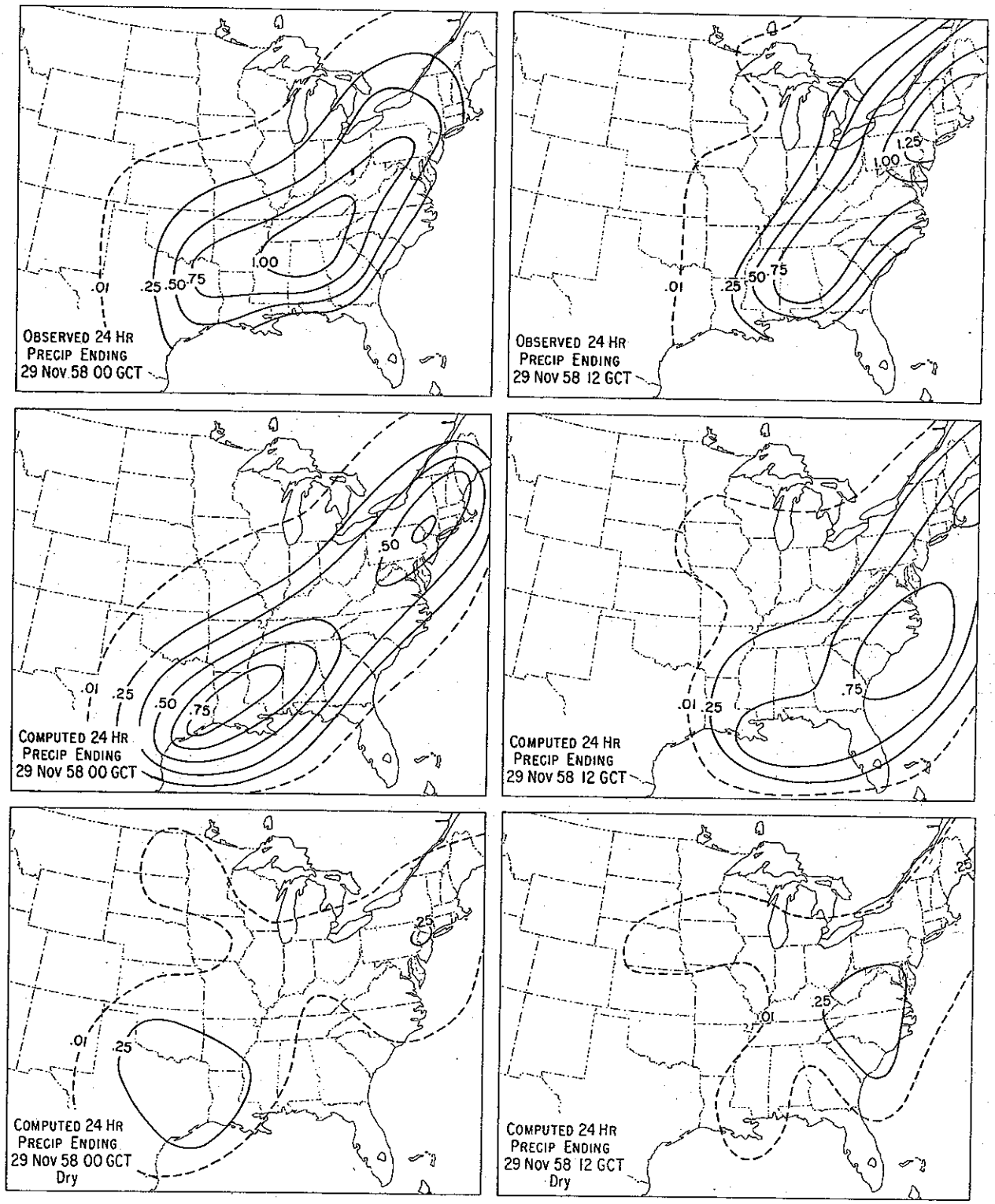

Fig. 10. Upper row: observed precipitation amounts; center row: forecast precipitation amounts obtained from the saturated-adiabatic model; lower row: forecast precipitation amounts obtained from the dry-adiabatic model. Unit: Inch.

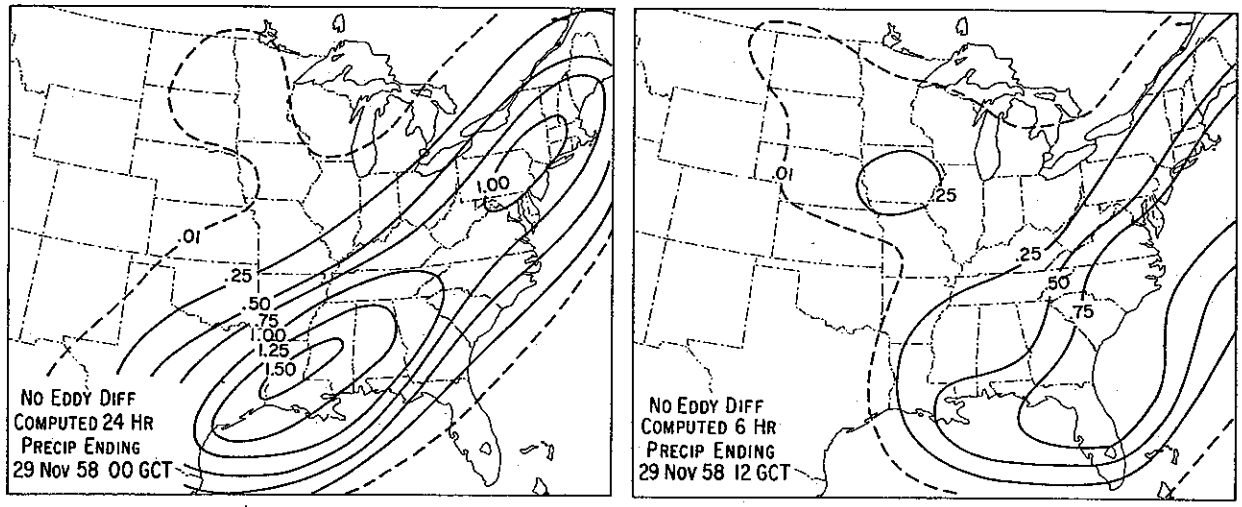

Fig. 11. Forecast 24-hour precipitation amounts applying the saturated-adiabatic model without lateral eddy diffusion.

In order to study the errors in the computed precipitation as a function of time, the 6-hourly precipitation amounts computed with the saturated-adiabatic model, together with the observed 6-hour amounts, are given in Figures 12 and 13. It is seen in both forecasts that, during the first 6-hour period, the computed amounts are somewhat too low. The reason may be that the area of saturation at the 700 mb level at the initial time is not the actual area over which condensation occurs. In the latter part of the 24-hour forecasting periods, the computed amounts are slightly larger than those observed. This is partly the result of the overestimation of the intensification of the cyclone. For the southern area, the over-calculation in precipitation may also be due to the assumption that the whole atmospheric column is saturated when saturation is reached at the 700 mb level.

6. Concluding remarks. In view of the simplifications applied in our model, the computed precipitation amounts are in surprisingly good agreement with those observed. The results confirm the conclusions of Smagorinsky and Smebye that the effect of released latent heat must be taken into account in order to predict the observed precipitation amounts. They also indicate that, for periods of about 24 hours, a quasi-geostrophic saturated-adiabatic model may forecast reasonably accurate precipitation amounts. For appreciably longer periods, however, ageostrophic motions and non-adiabatic effects seem to become increasingly important.

The dry-adiabatic model is consistent when the static stability is horizontally uniform and remains constant. It is interesting to note that if the consistency requirements are violated by letting the stability vary through the larger-scale systems, the accuracy of the short-range forecasts is increased.

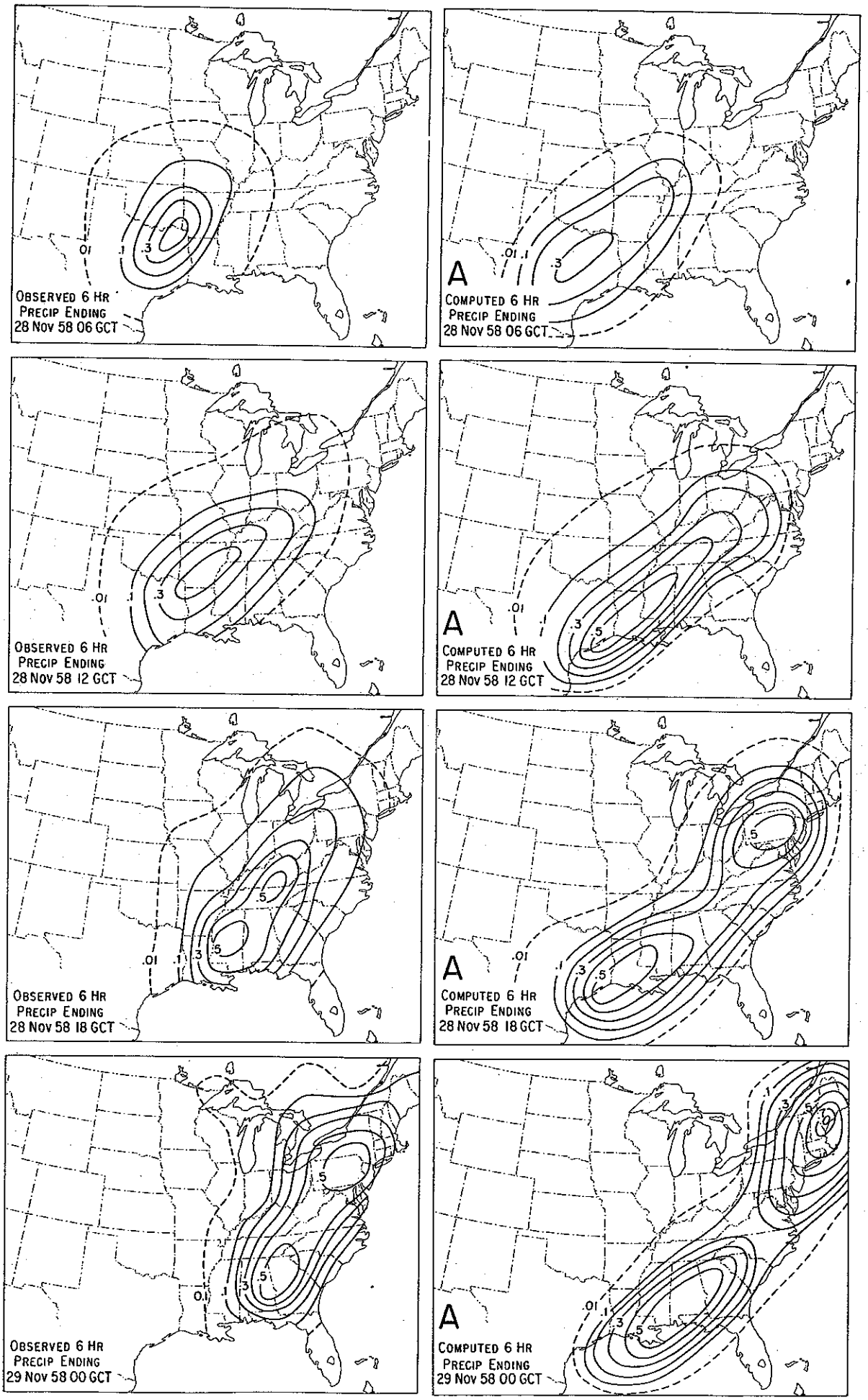

Fig. 12. Observed and forecast 6-hour precipitation amounts. Initial data 28 November 1958, 00 GCT.

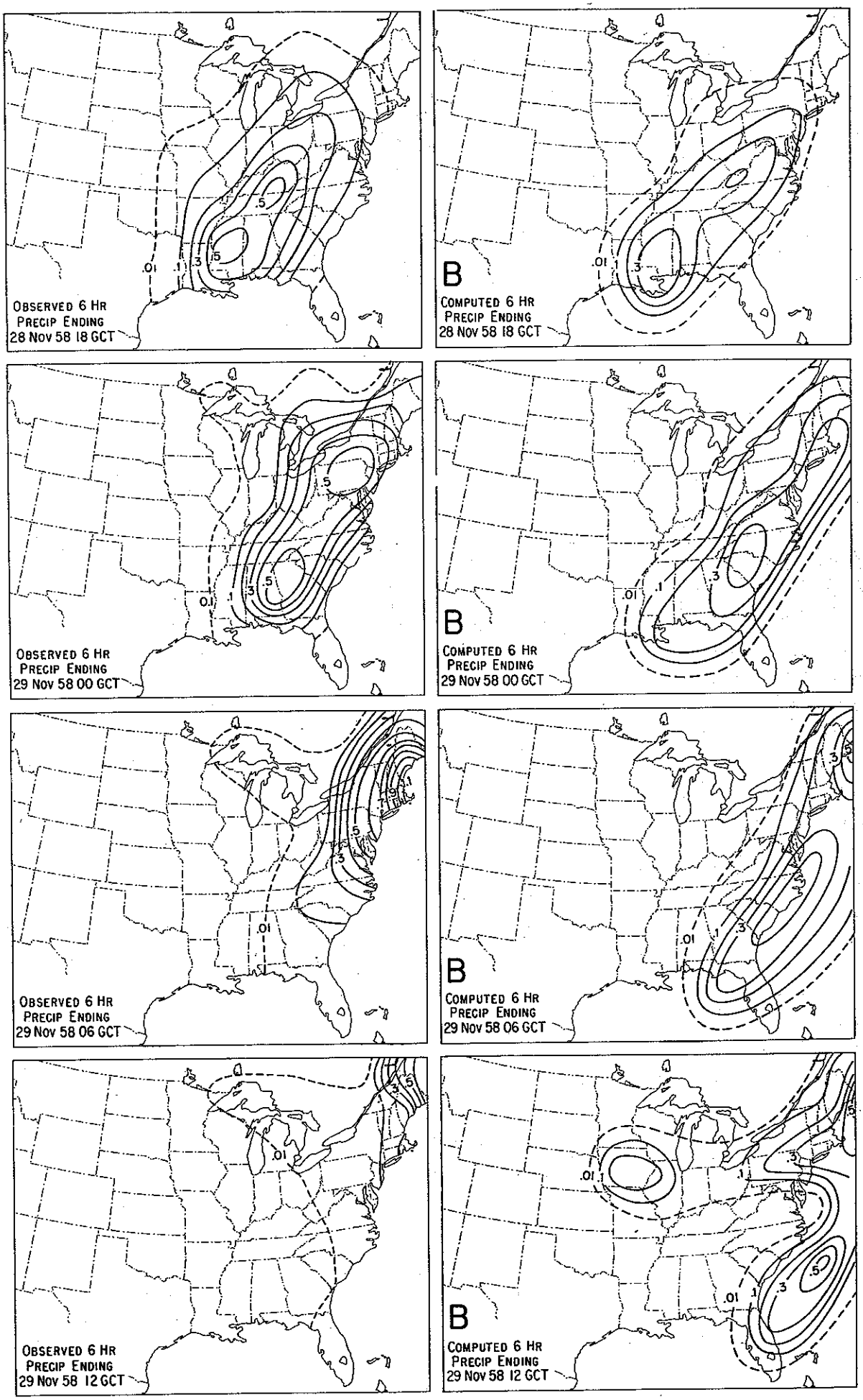

Fig. 13. Observed and forecast 6-hour precipitation amounts. Initial data 28 November 1958, 12 GCT.

Introduction of lateral eddy diffusion in the prediction equations improved the results by reducing the predicted precipitation amounts. The effect of the eddy diffusion terms was found to be particularly strong in cases where the horizontal scale of the condensation region was small.

Acknowledgement. The writer wishes to express his gratitude to Professor Sverre Petterssen for his advice and continuous encouragement throughout the course of this study.

LIST OF SYMBOLS

a wave number along the x-aksis.
b wave number along the y-aksis.
c_p specific heat of air at constant pressure.
f Coriolis parameter.
g acceleration of gravity.
H heat received by a unit mass per unit time.
L latent heat of evaporation (or sublimation)
p atmospheric pressure.
p_o 1000 mb.
Q_g aboslute geostrophic vorticity.
q_g relative geostrophic vorticity.
R specific gas constant of air.
r humidity mixing ratio.
r_s saturation value of r.
T temperature (°K).
T_d dewpoint temperature (°K).
t time.
$\boldsymbol{v}$ horizontal wind vector.
$\boldsymbol{v}_g$ geostrophic wind vector.
x, y horizontal coordinates.
Z height of isobaric surface.
α specific volume.
θ potential temperature.
σ $-(\alpha/\theta)(d\theta/dp)$ = a measure of static stability.
ω dp/dt = vertical velocity expressed in terms of pressure.
∇ the two-dimensional differential operator.
∇^2 the two-dimensional Laplace operator.

REFERENCES

AUBERT, E. F., 1957: On the release of latent heat as a factor in large scale atmospheric motions. *J. Meteor.*, **14**, 527—542.

CARLSTEAD, E. M., 1959: Forecasting middle cloudiness and precipitation areas by numerical methods. *Monthly Wea. Rev.*, **87**, 375—381.

CHARNEY, J., 1948: On the scale of atmospheric motions. *Geof. Publ.* **17**, No. 2.

ELIASSEN, A., and E. KLEINSCHMIDT, 1957: Dynamic Meteorology. *Handbuch der Physik* **48**, Berlin, p. 93.

ELIASSEN, A., 1959: On the formation of fronts in the atmosphere. *The Rossby Memorial Volume*, New York, 277—287.

FJØRTOFT, R., 1955: On the use of space-smoothing in physical weather forecasting. *Tellus*, **17**, 462—480.

HESSELBERG, T., 1915: *Veröff. Geophys. Inst. Leipzig*, 1.

HOLLMANN, G., 1956: Über prinzipielle Mängel der geostrophischen approximation und die Einführing ageostrophischer Windkomponenten. *Meteor. Rundschau*, **9**, 73—78.

LORENZ, E. N., 1960: Energy and numerical weather prediction. *Tellus*, **12**, 364—373.

MIHALJAN, J. M., 1962: The baroclinic instability of a "2½ dimensional model atmosphere" in which the upper level is non-divergent. *Tellus*, **14**, 116—122.

PETTERSEN, S., D. L. BRADBURY and K. PEDERSEN, 1961: The Norwegian cyclone models in relation to heat and cold sources. *Geof. Publ.*, **24**, 243—280.

RICHARDSON, L. F., 1926: Atmospheric diffusion shown on a distance-neighbour graph. *Proc. Roy. Soc., A*, **110**, 709—737.

RICHTMYER, R. D., 1957: Difference methods for initial-value problems. Interscience Publishers, Inc., New York, p. 101.

SMAGORINSKY, J., 1956: On the inclusion of moist adiabatic processes in numerical prediction models. *Ber. d. deutsches Wetterd.*, **38**, 82—90.

SMEBYE, S., 1958: Computation of precipitation from large scale vertical motion. *J. Meteor.*, **15**, 547—560.

WIIN-NIELSEN, A., 1959: On certain integral constraints for the time integration of baroclinic models. *Tellus*, **11**, 45—49.

INNHOLD

Avhandlinger som ønskes opptatt i «Geofysiske Publikasjoner», må fremlegges i Videnskaps-Akademiet av et sakkyndig medlem.

Vol. XX.

No. 1. B. J. Birkeland: Homogenisierung der Temperaturreihe Greenwich 1763—1840. 1957.
» 2. Enok Palm: On Reynolds stress, turbulent diffusion and the velocity profile in stratified fluid. 1958.
» 3. Enok Palm: Two-dimensional and three-dimensional mountain waves. 1958.
» 4. L. Vegard: Recent progress relating to the study of aurorae and kindred phenomena. 1958.
» 5. Leiv Harang: Heigth distribution of the red auroral line in polar aurorae. 1958.
» 6. Bernt Mæhlum: The diurnal- and sunspot-cycle variation of the layers *E*, *F*1 and *F*2 of the ionosphere as observed in Norway during the period 1932—1956. 1958.
» 7. Jonas Ekman Fjeldstad: Ocean current as an initial problem. 1958.
» 8. Olav Holt and Bjørn Landmark: Some statistical properties of the signal fine structure in ionospheric scatter propagation. 1958.
» 9. L. Vegard, S. Berger, and A. Nundal: Results of auroral observations at Tromsø and Oslo from the four winters 1953—54 to 1956—57. 1958.
» 10. Eigil Hesstvedt: Mother of pearl clouds in Norway 1959.
» 11. A. Omholt: Studies on the excitation of aurora borealis. I. The hydrogen lines. 1959.
» 12. G. Kvifte: Nightglow observations at Ås during the I. G. Y. 1959.
» 13. Odd H. Sælen: Studies in the Norwegian Atlantic current. Part I: The Sognefjord section. 1959.

Vol. XXI.

No. 1. A. Omholt: Studies on the excitation of aurora borealis II. The forbidden oxygen lines. 1959.
» 2. Tor Hagfors: Investigation of the scattering of radio waves at metric wavelengths in the lower ionosphere. 1959.
» 3. Håkon Mosby: Deep water in the Norwegian Sea. 1959.
» 4. Søren H. H. Larsen: On the scattering of ultraviolet solar radiation in the atmosphere with the ozone absorption considered. 1959.
» 5. Søren H. H. Larsen: Measurements of atmospheric ozone at Spitsbergen (78°N) and Tromsø (70°N) during the winter season. 1959.
» 6. Enok Palm and Arne Foldvik: Contribution to the theory of two-dimensional mountain waves 1960.
» 7. Kaare Pedersen and Marius Todsen: Some measurements of the micro-structure of fog and stratus-clouds in the Oslo area. 1960.
» 8. Kaare Pedersen: An experiment in numerical prediction of the 500 mb wind field. 1960.
» 9. Eigil Hesstvedt: On the physics of mother of pearl clouds. 1960.

Vol. XXII.

No. 1. L. Harang and K. Malmjord: Drift measurements of the E-lager at Kjeller and Tromsø during the international geophysical year 1957—58. 1960.
» 2. Leiv Harang and Anders Omholt: Luminosity curves of high aurorae. 1960.
» 3. Arnt Eliassen and Enok Palm: On the transfer of energy in stationary mountain waves. 1961.
» 4. Yngvar Gotaas: Mother of pearl clouds over Southern Norway, February 21, 1959. 1961.
» 5. H. Økland: An experiment in numeral integration of the barotropic equation by a quasi-Lagrangian method. 1962.
» 6. L. Vegard: Auroral investigations during the winter seasons 1957/58—1959/60 and their bearing on solar terrestrial relationships. 1961.
» 7. Gunnvald Bøyum: A study of evaporation and heat exchange between the sea surface and the atmosphere. 1962.

Vol. XXIII.

No. 1. Bernt Mæhlum: The sporadic E auroral zone. 1962.
» 2. Bernt Mæhlum: Small scale structure and drift in the sporadic E layer as observed in the auroral zone. 1962.
» 3. L. Harang and K. Malmjord: Determination of drift movements of the ionosphere at high latitudes from radio star scintillations. 1962.
» 4. Eyvind Riis: The stability of Couette-flow in non-stratified and stratified viscous fluids. 1962.
» 5. E. Frogner: Temperature changes on a large scale in the arctic winter stratosphere and their probable effects on the tropospheric circulation. 1962.
» 6. Odd H. Sælen: Studies in the Norwegian Atlantic Current. Part II: Investigations during the years 1954-59 in an area west of Stad. 1963.

Vol. XXIV.

In memory of Vilhelm Bjerknes on the 100th anniversary of his birth. 1962.

A.s John Griegs Boktrykkeri